V963 Persei as a Contact Binary

Joel A. Eaton
7050 Bakerville Road, Waverly, TN 37185; eatonjoel@yahoo.com

Gary W. Steffens
Morning Star Observatory, Tucson, AZ; gwsteffens@yahoo.com

Andrew P. Odell
Northern Arizona University, Flagstaff, AZ 86011; deceased, May 10, 2019

Received October 1, 2020; revised October 4, 2021; accepted November 3, 2021

Abstract We have reanalyzed V963 Persei, a close binary star which R. G. Samec claimed to have components with very similar masses ($q = M_2 / M_1 = 0.87$), finding that the mass ratio is actually $q \approx 0.35$. The system seems to be marginally in contact with a large temperature difference between the components, similar to a class of binaries analyzed by Kałużny. Primary eclipse is a complete transit, and the peculiarities of the light curve and, more particularly, its changes, are best explained by a cool spot on the more massive component and a hot spot on the less massive one. We classify the spectrum as F9–G1, present radial velocities for both components, and analyze the light curves for various combinations of cool and hot spots. The system overfills its Roche lobe in all our solutions, but the degree depends uncomfortably on assumptions about spottedness. The masses are $M_1 = 1.60 \pm 0.50$ and $M_2 = 0.54 \pm 0.20$ $M_\odot$. Finally, we discuss limitations on our ability to determine properties of contact binaries and the apparent absurdity of some of our results.

1. Introduction

We became interested in the close binary V963 Per (GSC 3355 0394; $m_B \approx 13.2$) as an analogue of the star W Crv (Odell 1996; Ruciński and Lu 2000), a close possibly-contact system with components of decidedly different effective temperature, but with a masses uncharacteristically similar to one another for such a system. Samec *et al.* (2010a, b; hereafter SAMEC) had obtained photometry of this faint binary on two nights and analyzed the light curve, finding a transit primary eclipse and a mass ratio $q = M_2 / M_1 = 0.8731$. In their solution the eclipses were partial. The secondary eclipse (of the cooler, less-massive star), however, seemed to show phases of second and third contact, as though it were total.

Given its period and the shape of its light curve, this star would seem to belong to a class of close binaries with large ellipsoidal variation, transit primary eclipses (larger, more massive star eclipsed), and a temperature difference much larger than in the typical cool contact binary (W UMa binary). See Kałużny (1983, 1986a–d; Kałużny and Pojmański 1983) for a comprehensive discussion of these stars. The large temperature difference is unexpected for a binary in physical contact, for which the first-order theory of structural stability predicts a rather uniform surface temperature (Lucy 1967, 1968a, b). In addition, these stars show unexpected waves in their light variation, brightness increasing from phase zero (primary eclipse) to phase 0.5 (secondary), like the sine-theta phase variation of the well-known reflection effect. And there is usually a difference in brightness between phases 0.25 and 0.75, with phase 0.75 usually fainter and much more variable.

The unexpected sine-theta variation may be explained in a number of rather different ways depending on one's proclivities and the fashion of the day. Kałużny reproduced it in his analyses with an elevated reflection effect, acknowledging that he was using a high albedo merely as a fitting parameter, not claiming that the effect was actual reflection. A number of us have implicitly taken this approach in fitting close binaries. Another way of fitting the queer phase dependence is putting a rather large dark spot on the hemisphere of the primary (more massive) component facing the secondary. This reflects the notion that cool magnetic spots might be expected in these rapidly rotating stars. A third alternative is to use a bright spot on the inner face of the secondary, which might result from mass flowing onto it from the primary (e.g., SAMEC, section 5). Both of these uses of a spot imply some sort of temperature gradient through the neck region of the binary. In fact, postulating a smooth variation of local effective temperature through this region gives a surprisingly good representation of the data. Speculating, we may imagine that it has to do with the energy-transfer mechanism in this sort of star.

We have reobserved V963 Per, obtaining extensive photometry (see Odell *et al.* 2011; hereafter ODELL) and the first spectra suitable for measuring radial velocities. The high quality of the photometry challenges us to analyze the light variation both to fit it definitively at a single epoch and to explore the physical mechanisms for its variation. The light curve is variable, and our data for 2010–2011 define a change that we will use to test ideas about what produces such variability. The spectra measure the velocity amplitude of the primary, clearly detect the secondary, and constrain the mass ratio. They also give a much clearer determination of the spectral type of the primary star than SAMEC could infer from colors.

A second reason for analyzing this star was our concern with the quality of SAMEC, a paper with rather many errors, both careless and substantive. The most egregious of these sins of publication have been discussed by ODELL, but we can now comment on the light curve solution. It turns out that the mass ratio of this binary is not the large value found by SAMEC

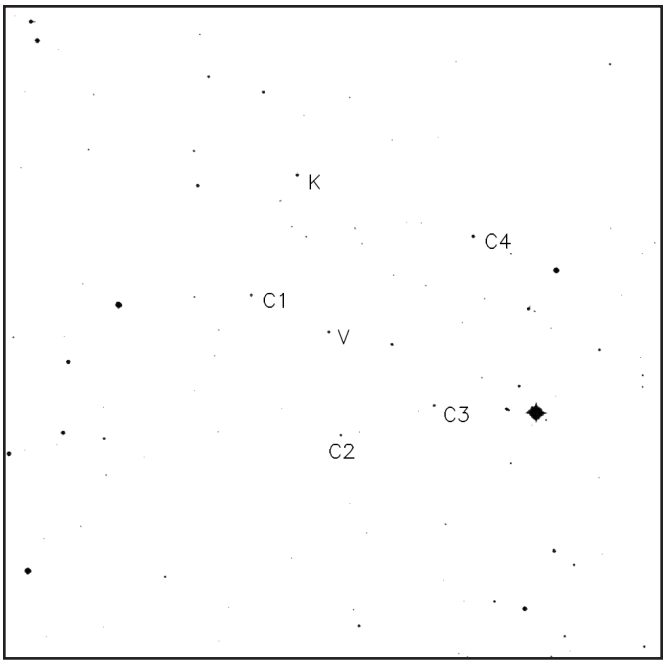

Figure 1. Comparison stars used. This is a 20 × 20 arcmin. field from the red Palomar Sky Survey; N to top, E to left. V963 Per is marked with a V; we used the four numbered stars plus the check star, K, for our five comparison stars. This check star was SAMEC's comparison.

but a much smaller one more consistent with those of similar binaries. The late spectral type found by SAMEC is also wrong, probably as a result of neglecting interstellar reddening.

We have adopted the following ephemeris for our analysis:

$$\text{HJD(Obs)} = 2455563.6833 + 0.462078\varphi, \qquad (1)$$

φ being the phase, as determined by ODELL.

2. Observations

Our observations consist of both precise photometry and moderate-dispersion spectra. Odell obtained photometry on four nights in late 2010 (11–13 and 29 Dec. UT) and seven nights in early 2011 (5, 9, 11, 15, 16 Jan. and 9 and 26 Feb. UT). We are dividing these observations into two groups, the first for 11 Dec.–3 Jan, which we call 2011-dec, and the second for 5 Jan.–9 Feb., which we call 2012-jan. We are omitting the night of 26 Feb. from our photometric analyses because it fell noticeably below the data for 2012-jan. These data have been published in ODELL and are some of the most precise measurements ever made for a star of this type. Steffens has recently observed it again (28–30 Oct. and 1 Nov. 2019 UT), getting a light curve for 2019-oct. This photometry consists of differential magnitudes measured with the usual commercially available BVR_cI_c filters; they are not transformed to the standard system via observations of standard stars. Since the variable and comparison stars were all on the same CCD images, we have not corrected them for differential extinction, either. We used the same five comparison and check stars as ODELL (see Figure 1). There are roughly 226, 234, and 306 data in each color for the three epochs 2011-dec, 2012-jan, and 2019-oct, respectively. The data for 2019 are available from the AAVSO ftp archive as the ASCII file Eaton-492-V963Per.txt at ftp://ftp.aavso.org/public/datasets/. Listed are the Reduced Julian Date (RJD = HJD-2400000) of observation, and differential magnitudes of the variable and check stars for the four passbands. This dataset is identified by the symbol 2019-oct at the end of each line. Entries with missing data are identified with magnitudes equal to 99.999.

The spectra come from the Steward Observatory 90-inch telescope and Meinel spectrograph. We took 25 spectra of V963 Per covering the range 4750–5300 Å at a resolution of

Table 1. Measured Radial Velocities for V963 Per.

RJD	*Phase*	RV_1	RV_1
2455580.6581	0.7360	35	—
2455580.6722	0.7663	17	—
2455580.6937	0.8128	43	—
2455580.7077	0.8431	24	—
2455580.7336	0.8994	17	—
2455580.7476	0.9295	8	—
2455580.7985	0.0396	–152	—
2455580.8124	0.0697	–100	—
2455580.8372	0.1236	–125	—
2455580.8515	0.1543	–160	—
2455583.6220	0.1500	–157	—
2455583.6359	0.1802	–134	—
2455583.6566	0.2249	–171	—
2455583.6705	0.2550	–170	—
2455583.6908	0.2990	–169	—
2455583.7048	0.3293	–160	—
2455583.7268	0.3769	–131	—
2455583.7407	0.4070	–143	—
2455583.7613	0.4515	–105	—
2455583.7819	0.4961	–71	—
2455583.7959	0.5264	–61	—
2455583.8267	0.5931	–5	—
2455583.8407	0.6234	–1	—
2455583.8618	0.6990	–4	—
2455583.8758	0.6993	18	—
2455931.6137	0.2517	–147	173
2455931.6277	0.2820	–147	178
2455931.6761	0.3868	–120	113
2455931.6901	0.4171	–115	69
2455931.7128	0.4662	–87	—
2455931.7269	0.4967	–75	—
2455931.7516	0.5501	–49	—
2455931.8448	0.7518	19	–213
2455931.8589	0.7824	18	–247
2455931.8812	0.8306	1	—
2455931.8953	0.8611	2	—
2455931.9183	0.9109	–11	—
2455931.9323	0.9412	–9	—
2455931.9645	0.0109	–165	–11
2455937.8126	0.6670	18	–200
2455937.8267	0.6975	17	–243
2455937.8657	0.7819	3	–255
2455940.8276	0.1919	–136	172
2455940.8487	0.2375	–151	142
2455940.8698	0.2832	–159	161
2455940.8904	0.3278	–157	96
2455940.9108	0.3719	–138	66
2455966.6535	0.0826	–126	—
2455966.6759	0.1311	–136	—
2455966.6939	0.1701	–155	116
2455966.7145	0.2146	–160	149
2455967.5918	0.1132	–135	—

roughly R = 5000, on 2 nights (19 and 22 Jan. UT) in 2011. All of the exposures were 1200 s, 0.03 phase. We then bagged 27 more spectra in 2012 (5, 11, and 14 Jan. and 9 and 10 Feb. UT) covering the wavelength range 4050–4950 Å with a new CCD, which gave much better signal-to-noise and has allowed us to isolate the spectrum of the faint secondary component. See Table 1 for dates and measured velocities.

Spectral Type SAMEC inferred a spectral type around K2 from the color of the system. This is much later (cooler) than expected for a binary with the light curve and period of V963 Per (e.g., Qian *et al.* 2017, Figure 10). In fact, the relative strengths of the Hβ and Mg I b lines in our spectra for 2011 are inconsistent with such a cool star. Instead, they imply a type near G0. The newer spectra for 2012 lead directly to a similar classification, namely F8–F9, but certainly no later than G0.

Radial Velocities of the Components The spectra for 2012 have high enough S/N (and resolution, 43 km/s/pixel) that we could isolate profiles of both components in cross-correlation functions derived from them. These are based on the metallic lines between Hγ and Hβ, and exclude the H lines and G band. Figure 2 shows an example of an IRAF session (splot) in which Odell has fit a Gaussian to the profile of the primary component. It shows the averaged line profile (cross-correlation function with the G0 V star HD 50692 as the template) for one of these spectra, showing the relative strengths of the lines in the two components of the system. There Odell was fitting Gaussians to the blended profile with IRAF to get the velocity shifts of the stars.

Errors of the velocities deduced from fitting the profiles with IRAF are 10 km s^{-1} for the primary and 40 km s^{-1} for the secondary. Sine curves fit to the velocities give semiamplitudes of $K_1 = 88.7 \pm 2.6$ km s^{-1} and $K_2 = 199 \pm 6.7$ km s^{-1} for the components (see Figure 3). For 2011, $K_1 = 104 \pm 4.7$, so that a mean amplitude for both years is $K_1 = 92.3 \pm 2.4$ km s^{-1}. These values show that the mass ratio is likely no larger than $q = M_2/M_1 = 0.46$. However, the systemic (γ) velocities of the stars differ by 20 km s^{-1} in the sense of secondary's velocities after phase 0.5 being too positive. If we require both stars to have the same γ velocity and assume the secondary's velocities after secondary eclipse are discordant, we get $K_2 = 219$ km s^{-1} and $q < 0.42$, the inequality reflecting the effect that the expected hot spot on the inner face of the secondary would have on its measured velocity. Fitting light curves using the Wilson-Devinney code gives an even smaller photometric mass ratio, roughly 0.34 (section 4.2 below), which allows for the asymmetrical surface-brightness distribution on the secondary. This small q is consistent with the relative strengths of the line components (Figure 2). Indeed, the line profiles require it, both because of the relative strengths of the components' profiles and because the hot spot on the inner face of the secondary biases the velocity-curve solution to smaller K_2. A large mass ratio, such as the 0.87 from SAMEC, is not consistent. Thus q is < 0.4, and the system is roughly as we argued in the Introduction.

3. Ephemeris

We now have enough times of minimum for this sparsely observed system to begin to define its period and look for changes in it. Table 2 lists all the times of minimum we have found and derived. In addition to the times measured by ODELL, we have added five that Odell derived from archival SWASP (Butters *et al.* 2010) data, the one from SAMEC, four more from the literature, and four measured by Steffens. See Table 2; uncertainties listed represent measurement only, not the potentially much larger ones caused by distortions of the light curve.

The times from Odell and Steffens were determined graphically. They entered the data for a minimum in a spread sheet, plotted them for an assumed time of minimum, replotted them reflected about that time, and adjusted that assumed time of minimum until the direct and reflected data lined up to the eye. This procedure relies on the averaging qualities of human perception. However, it does not give an uncertainty; this we estimate from our experience in fitting times of minimum of GSC 3208 1986 with the Wilson-Devinney code (Eaton *et al.* 2019).

The point from SAMEC deserves a further comment. That paper listed four times of primary minimum, which we could not identify with any of the times of observation given. We think it likely that the times of observations listed are bogus as

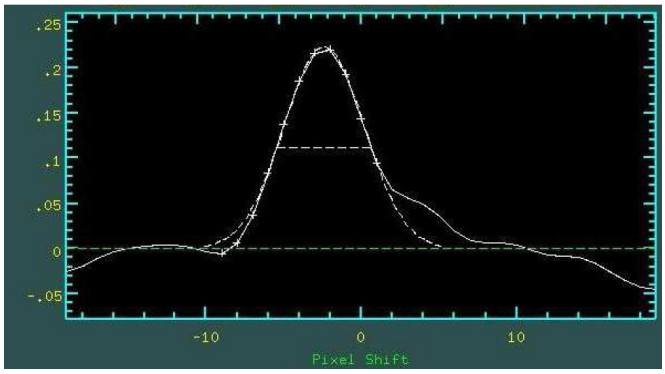

Figure 2. Part of a screen shot of an IRAF session showing the decomposition of the profile at quadrature, phase 0.25 (first entry in Table 1). Notice the difference in the strength of the profiles of the two stars.

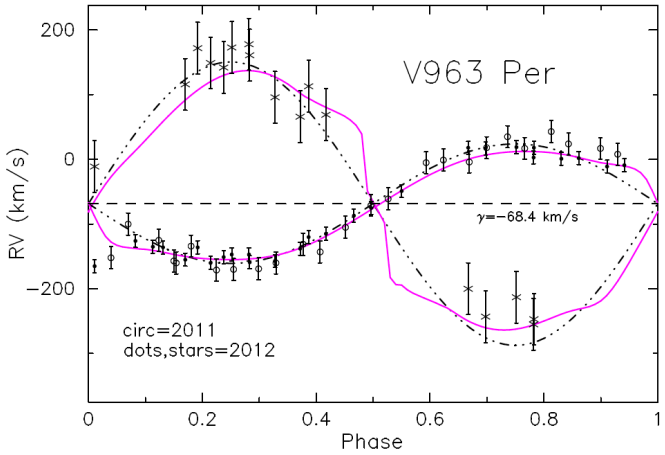

Figure 3. Velocity curves for V963 Per. Dots and stars are data from 2012 for the primary and secondary, respectively. Circles are data from 2011 for the primary. Dash-dotted (black) curves are sine curves fit to the data as described in section 2, $K_1 = 92.3$, $K_2 = 219$, and $\gamma = -68.4$ km s^{-1}. Solid (magenta) curves are fits from WD mentioned in section 4.1.4.

Table 2. Times of Minimum for V963 Per.

RJD	*σ*	*Epoch*	*(O–C)*	*Source*
2454363.6680	0.003	–2597.0	0.0013	S-Wasp
2454381.6950	0.003	–2558.0	0.0072	S-Wasp
2454407.5700	0.003	–2502.0	0.0059	S-Wasp
2454438.5200	0.003	–2435.0	–0.0034	S-Wasp
2454439.4500	0.003	–2433.0	0.0025	S-Wasp
2454828.9913	0.0025	–1590.0	0.0120	Samec (2010a, b)
2455563.6834	0.0004	0.0	0.0001	Odell (2011)
2455564.6077	0.0004	2.0	0.0002	Odell (2011)
2455576.6211	0.0004	28.0	–0.0004	Odell (2011)
2455601.5749	0.0004	82.0	0.0012	Odell (2011)
2455618.6717	0.0004	119.0	0.0011	Odell (2011)
2455922.2549	0.0003	776.0	–0.0009	Banfi (2012)
2455923.6407	0.0005	779.0	–0.0014	Banfi (2012)
2455947.6703	0.0005	831.0	0.0002	Diethelm (2012)
2456312.7041	0.0005	1621.0	–0.0076	Diethelm (2013)
2457060.8021	0.0004	3240.0	–0.0139	Steffens
2458784.7950	0.0004	6971.0	–0.0340	Steffens
2458785.7197	0.0004	6973.0	–0.0335	Steffens
2458788.9544	0.0004	6980.0	–0.0333	Steffens

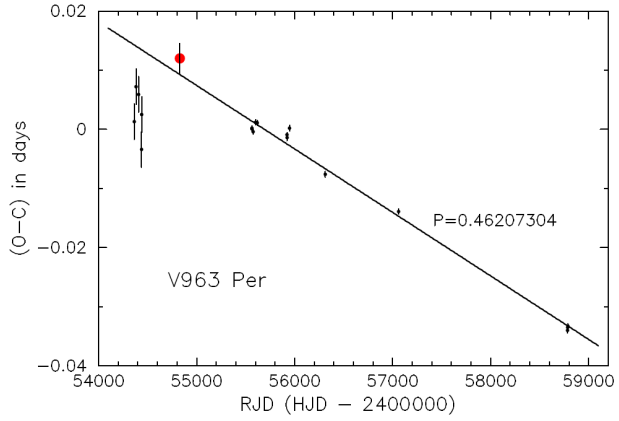

Figure 4. Times of primary minimum for V963 Per. This figure shows deviations of measured times of primary minimum from the linear elements of Equation 1. The large red symbol is the point from SAMEC discussed in the text, and the fitted line gives the revised period of Equation 2.

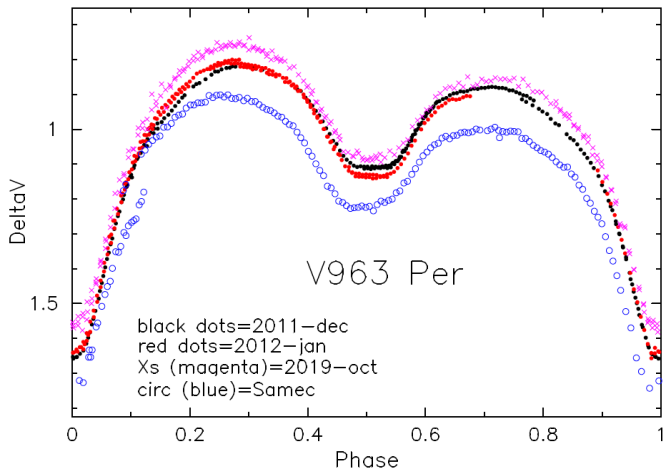

Figure 5. Visual light curves of V963 Per for four epochs. The difference between 2011 and 2012 probably results from a mismatch of the photometric bands; the lower general level for SAMEC (2008-dec), from variation of the comp star.

described in ODELL and section 4.1 below. The time listed in Table 2 is the one likely legitimate one.

The deviations of these measured times from Equation 1 (Table 2, column 4; Figure 4) do not show any trends implying a period change. Fitting a line to them gives the slightly improved elements of Equation 2.

$$HJD(Obs) = 2455563.6847(1) + 0.46207304(4)\varphi. \quad (2)$$

4. Analysis of the light curve

We have analyzed the light curves with the Wilson-Devinney (WD) code (2015 version; see Wilson and Devinney 1971; Wilson 1990, 1994; Wilson and Van Hamme 2015) because it allows spots at arbitrary positions on the components of a contact binary. This is important because the light curves of V963 Per and similar stars tend to be asymmetric, as though parts of the surface are hotter or cooler than expected in the standard picture of a binary system. In particular, phases either side of phase 0.5 are brighter, when the side of the smaller secondary star facing the larger primary is most exposed. This implies the secondary has either a bright spot on its neck facing the primary, or a dark (cool) spot on its rump facing away. Alternatively, there could also be a dark spot on the neck of the primary facing the secondary, although one does not show up in Doppler profiles of W Crv (Eaton *et al.* 2021). The system also shows a pronounced O'Connell Effect, being fainter by roughly 0.10 mag at phase 0.75 than at phase 0.25; that feature was roughly the same at all four epochs (Figure 5).

Practically all modern solutions of light curves are based on a standard Roche model in which the stars' surfaces are represented as gravitational equipotentials, Ω, in a system of two synchronously rotating centrally condensed masses. Surface brightnesses in this model are determined by theoretical limb- and gravity-darkening laws (parameters x_i and g_i) and some average or reference temperature for each component, T_i, with the mutual irradiation of the stars (reflection effect; bolometric albedos A_i) handled with schemes of varying sophistication.

Stars like V963 Per do not fit this model, in two ways. First, observationally, they show variations in brightness that the model cannot produce (see Figure 5). Second, theoretically, if they are contact binaries transferring luminosity through flows in a common envelope, they are not strictly in hydrostatic equilibrium and must have gravitational heads or other pressure gradients to drive and regulate these flows. So one must modify the standard model by using physical intuition to figure out how the star differs from our normal assumptions. As we explained in our Introduction, there are various ways to account for both the unexpected sine-theta wave in the light variation and the difference in brightness between phases 0.25 and 0.75. We could represent the former directly as a gradient in effective temperature through the neck, the details of the gradient based on some theory energy transfer in a contact binary. This works to first order; we have coded such a gradient into a program of Eaton's—see Figure 6. However this approach is not coded into the rather opaque WD program, so we would have to simulate it with a combination of dark and bright spots.

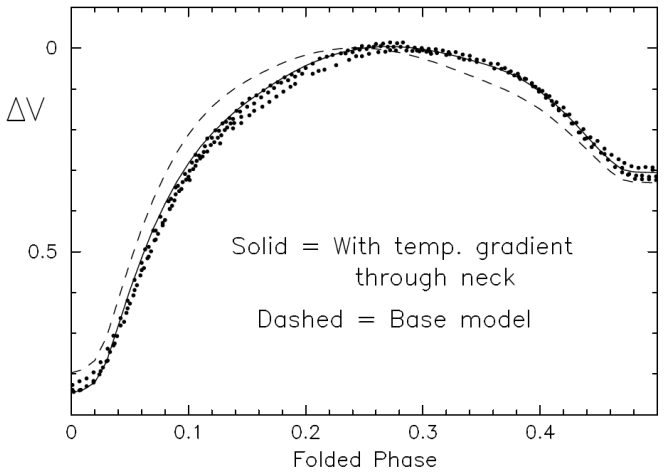

Figure 6. Light curve for a contact binary with a smooth temperature gradient through the neck between the components. Surface temperature assumed varies linearly with distance along the line between the stars between the centers of mass, between the reference temperatures for the two stars.

The difference in level between phases 0.25 and 0.75 likewise requires guesses about what produces it. It probably reflects spots of some sort on one of the stars. Furthermore, since the phenomenon seems to be common to this class of stars (see the papers by Kałużny), such spots must be a common property of the class. Are they dark spots on the trailing hemisphere of the larger, more massive primary star or bright spots on the trailing hemisphere of the secondary? Or, perhaps, dark spots on the leading hemisphere of the secondary? We suspect dark spots on the primary for two reasons: the light around phase 0.25 is relatively constant and the primary contributes most of the system's light, as well as the light variation during secondary eclipse when the smaller star is covered.

Furthermore, we have the challenge of explaining changes in light curves on surprisingly short timescales. This has become particularly acute with the very precise observations for this star by ODELL, reduced with meticulous care to minimize systematic errors between nights, in which changes cannot be dismissed as easily as those in other, less extensive or carefully handled data of this and similar stars. Observations around secondary eclipse over three consecutive nights in December 2010 showed variation of no more than 0.5 to 1%, yet data for a mere month later were consistently about 3 to 4% fainter in mid-eclipse, when only the larger primary component was visible (see Figure 5 and Figure 2 of ODELL). That change cannot be caused simply by a variable comparison star, since ODELL used an ensemble of *five* comparison stars whose relative brightnesses did not change materially.

What parameters, then, can one expect to change on timescales short enough to matter? Some properties, such as the masses, period, semi-major axis, and inclination must be constant on any timescales of interest in fitting seasonal light curves. Except in a few rather special circumstances, if these properties must change to fit two light curves of the same star, we know the physical model of the system is simply wrong. Other properties might change on various thermal or even dynamical time scales. Changes with timescales of order 10^7 years, such as the putative long-term period changes of many close binaries, correspond to the thermal timescale of a solar-type star. Thermal timescales of the outer layers of such stars, however, can be much shorter. Dynamical timescales might be of the order of a day for gas in a star's atmosphere ($R_\odot$ divided by the 10 km s^{-1} sound speed); less for flows in any free space around the binary components. The levels and timescales of variation in these stars imply that their atmospheres are quite dynamic, as Ruciński (2015, 2020) found in high-dispersion spectra of AW UMa and epsilon CrA, W UMa systems with rather deep common envelopes.

Tests of Program To get a better idea of possible systematic errors in the mass ratio derived with the Wilson-Devinney program, we calculated a light curve for W UMa with the Eaton code (Eaton 1986b, 1991; Eaton *et al.* 1993), with a point at every 0.01 phase, and fit that theoretical light curve with the WD code. The main difference between the two programs seems to be how they handle the reflection effect. Both programs gave the same light variation to within 0.001 mag but with slightly different albedos ($A_1=A_2=0.5$ for Eaton, $A_1=0.33$ and $A_2=0.47$ for WD). However, when we adjusted the properties by differential corrections, the WD code found a mass ratio 0.425 vs. 0.448 in the input data. This would seem to caution against generally accepting the formal errors derived by WD as true errors of the elements. However, in a second test, we calculated another theoretical light curve with properties more like the star in question here ($q=0.35$, $f=5\%$, $i=85$, $g=0.32$, $T_1=5850$ K, $T_2=4853$ K, $x_V=0.53$, and $A=0.01$). In this case an adjustment of salient parameters (q, f, i, T_2, and L_1) with WD found a mass ratio of 0.3508, an inclination of 84.8, and a filling factor of 5.2% with residuals less than 1 mmag. The WD program found the assumed mass ratio to within 0.0008 when approaching from both higher and lower assumed starting points.

4.1. Application to V963 Persei

We have made several classes of solutions to test various ways of explaining the deviations of the light curves from predictions of the standard binary model. The possible combinations of complications remind us of Polonius' fatuous classification of various types of drama (*Hamlet*; Act 2, Scene 2). Suffice it to say there is a bewildering range of both cool and hot spots on both components, as well the use of a large albedo for the secondary. To limit this range, we will consider only two to three spots divided between the two component stars. Table 3 identifies the combinations of spots assumed and the properties derived.

We must fix some of the parameters of the model to theoretical values. Specifically, we adopted a temperature of the primary consistent with its spectral class, convective gravity darkening (Lucy 1967), convective reflection effect (Ruciński 1969), the Kurucz-atmospheres option in the WD code, and linear limb-darkening coefficients from van Hamme (1993) and al-Naimy (1978). Of course, those values of the limb-darkening coefficients might not apply to a star like V963 Per with likely spots on the inner, eclipsed face of at least one component.

Finally, we are concentrating on the two epochs for ODELL because they are on the same photometric system, somewhat less on our data for 2019-oct, and will attempt to fit the data from SAMEC for 2008-dec. These latter data are problematic

Table 3. V963 Per: Light-Curve Solutions.

Parameter	2011-dec	2012-jan	2019-oct	2008-dec	§4.1.2 Spots	Big A_2
i(°)	82.80(8)	82.96(13)	85.05(21)	83.12(fixed)	83.43(19)	83.07(11)
q(M_2/M_1)	0.3353(8)	0.3397(5)	0.3165(20)	0.3351(fixed)	0.3497(11)	0.3578(11)
Ω	2.522(2)	2.543(2)	2.464(5)	2.530(15)	2.569(3)	2.539(2)
fillout	9.9%	4.7%	19.5%	6.1%	2.2%	23.4%
T_1(K, fixed)	6000	6000	6000	6000	6000	6000
T_2(K)	3941(15)	4070(28)	4284(38)	3387(609)	3638(38)	4113(47)
A_2	0.5	0.5	0.5	0.5	0.5	4.15(5)
$<\sigma_{fit}>$	0.010	0.009	0.012	0.014	0.013	0.008
Spots on the More Massive Component						
long(°)	44(1)	47(2)	53(3)	45(4) & 180(4)	none	76.7(9)
rspot(°)	13.0(1)	7.9(6)	12.2(5)	15.2(7) & 13.7(7)		13.1(3)
T_{spot}/T_1	0.80	0.80	0.80	0.8 & 0.8		0.44(12)
Spots on the Less Massive Component						
long(°)	14.9(4)	38(1)	30(1)	17(4)	74(6) & 4(4)	none
rspot(°)	79(1)	90(1)	79(2)	78(7)	25(6) & 70(3)	
T_{spot}/T_2	1.303(4)	1.282(7)	1.235(9)	1.36(5)	1.27(90) & 1.36(9)	

Note: Numbers in parentheses are the errors of the last digits. All spots are assumed to be on the equator. Limb-darkening coefficients: $x_{1,2}(B) = 0.709, 0.866$, $x_{1,2}(V) = 0.573, 0.723$, $x_{1,2}(R) = 0.491, 0.623$, and $x_{1,2}(I) = 0.411, 0.523$, $<\sigma_{fit}>$ is the directly calculated average standard deviation, in mags, for all the data, weighted equally, not some arcane number calculated by WD.

for several reasons. It is not clear exactly when SAMEC even took them (their text says 2007–2008, but the dates in their data table correspond to 2008–2009), and we have identified a likely 1-day error in the times listed in their Table 1 (ODELL). This is all consistent with the allocations of observing time to various authors of SAMEC. On further reflection, the data for B and V seem to have a curious shift in phase between their first and second night which cannot be explained by another 1-day error or by using the wrong orbital period. We suspect the data for the first night do not have a heliocentric correction applied to them. Applying one (0.0046 d.) tightens up the phasing considerably. This effect is not apparent in their Figures 2, 4, and 5 because of these plots' small scale and use of rather large symbols. Furthermore, their published data for R and I do not agree with those for B and V, since they seem to be intensities, not magnitude differences as advertised. We suspect the B and V data came from an incomplete earlier reduction of the data than the R and I data. This is all judicious speculation; however, correspondence with the authors in 2010–2011 failed to obtain a coherent data set. Consequently, we have decided to use only the B and V data, reducing the published Julian Dates by one day and adding 0.0046 d. to the times for their first night. These are the light curves in Figure 8.

4.1.1. Cool primary spot/hot secondary spot

This approach represents the present canonical model for such stars. We placed a cool spot on the primary component to account for the O'Connell effect and a hot spot on the inner face of the secondary to account for the sine-theta variation. See columns 2 to 5 of Table 3 and Figures 7 and 8. The solutions fit as well as expected given the variability of the light curve and the limitations of our knowledge about these stars. The measured values for q and i agree quite well for 2011-dec and 2012-jan, somewhat less so for 2019-oct. The fit for 2008-dec (SAMEC) is much worse, and we could not begin to fit the upward slope of the apparently total phases of secondary minimum.

4.1.2. Two hot spots on secondary

The rationale for this combination, that both the sine-theta wave and the O'Connell effect are caused by heating of the cooler secondary component, comes from our finding that the secondary of W Crv has hot material on both its leading and trailing sides and that this shows up as lots of extra light throughout the orbit of that star (van Hamme and Cohen 2008). Our solution for 2011-dec is given in Table 3, column 6 and plotted in Figure 9. The fit around secondary eclipse, of the spotted star, is noticeably worse than for the more symmetrical secondary component in section 4.1.1. The fit for 2012-jan is somewhat better ($<\sigma_{fit}> = 0.009$). The change in T_2 between 2011-dec and 2012-jan is roughly +400 K, likely reflecting a drop in the brightness of the primary. Such a temperature change seems unlikely on such a short timescale, making a hot O'Connell spot unlikely.

4.1.3. Cool primary spot/big A_2 for secondary

We are looking at this approach because it worked for Kałużny and because it gives us a way to see how a spot with a different temperature distribution than assumed by WD might improve the solutions. Our solution for 2011-dec is given in Table 3, column 7 and plotted in Figure 10. This situation here is similar to section 4.1.1 but with a hot spot whose brightness is more centrally peaked. This concentration of intensity gives the noticeably steeper partial branches of secondary eclipse seen around phase 0.4 in Figure 10. Our tentative conclusion is that the spots are not likely to be so centrally bright as in this approach, a situation that might be expected of a flow away from the neck between the stars, cooling as it goes.

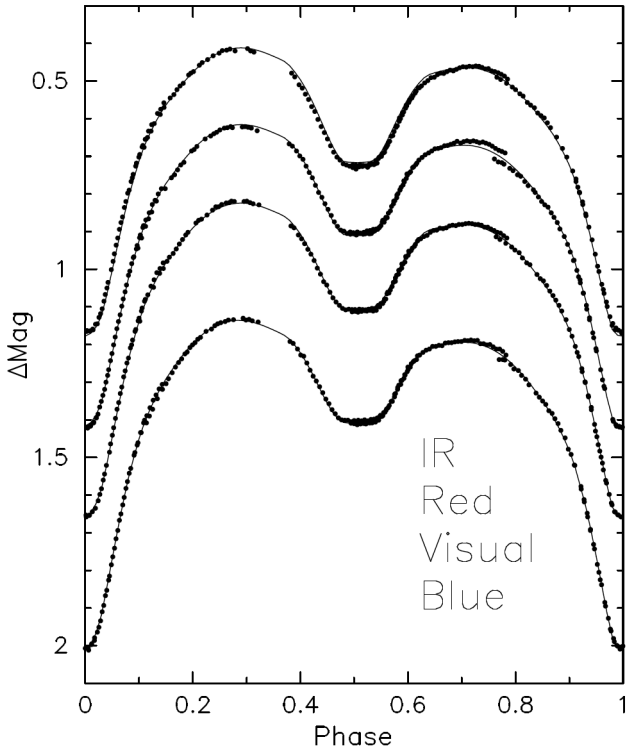

Figure 7. Light curve fit for 2011-dec with a hot spot on the secondary and a dark spot on the primary. This is the solution from column 2 of Table 3.

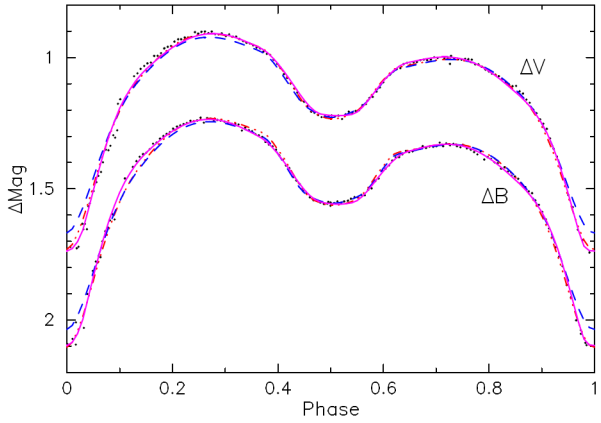

Figure 8. Three "solutions" for 2008-dec. The dots are the photometry from SAMEC, massaged as described in section 4. The magenta solid line is our solution (column 5 of Table 3), the blue dashed line, our representation of SAMEC's solution as a transit, and the dotted-dashed red line, our representation of their solution as an occultation.

4.2. Properties of the stars

We can estimate the masses of the components from a simultaneous solution of the light curves (2011-dec) with the reasonably well determined velocity curve of Star 1 for 2012 ($a = 3.23 \pm 0.36\,R_\odot$ for $q = 0.336$, $M_1 = 1.60 \pm 0.50$, $M_2 = 0.54 \pm 0.20\,M_\odot$, and $R_1 = 1.56 R_\odot$). The luminosity of the primary star would be $2.8 \pm 0.6\,L_\odot$. These values are roughly consistent with calculations for a 1.2–1.3 $M_\odot$ star in the main sequence to give the observed luminosity and radius (Girardi *et al.* 2000). Models in this range with the right luminosity and radius are all younger than the Sun, which suggests, weakly, that the primary may have grown through mass exchange (cf. Ruciński and Lu 2000).

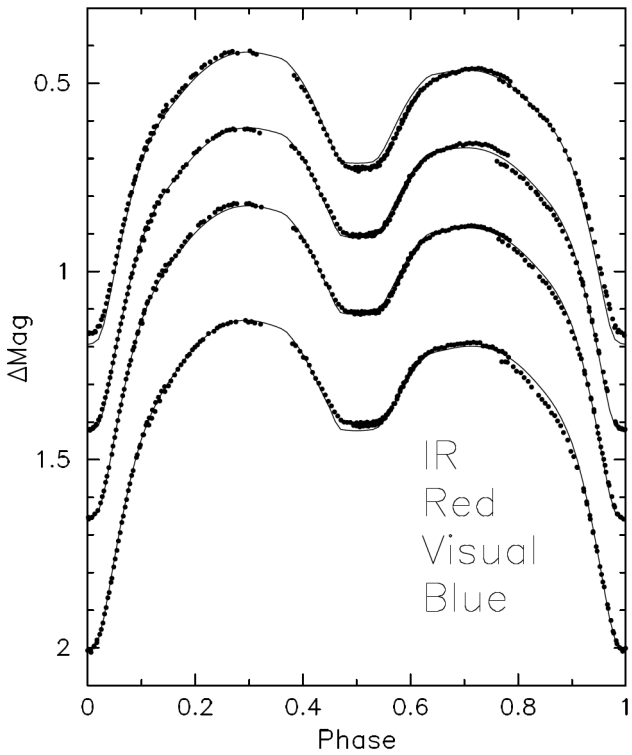

Figure 9. Light curve fit for 2011-dec with two hot spots on the secondary. This is the solution from column 6 of Table 3.

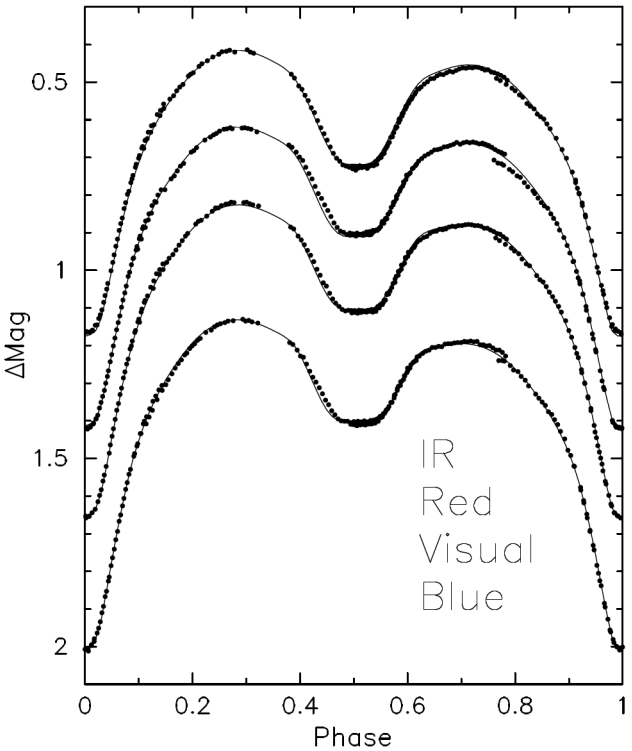

Figure 10. Light curve fit for 2011-dec for a secondary with a largeA2 and a cool spot on the primary. This is the solution from column 7 of Table 3.

5. Implications for contact binaries

Binaries with surfaces enclosed in a common envelope present a problem, both observationally and theoretically. To understand V963 Per we must consider just how it fits into the context of contact binaries as a class. First-order theory holds that these stars would be enclosed in a common gravitational equipotential surface whose local temperature is determined by gravity darkening and a weak reflection effect (Lucy 1967), a surface of roughly constant surface brightness. Warmer contact binaries with possibly radiative envelopes seem to fit this expectation, but the cooler ones with convective envelopes do not. In this latter group, Binnendijk's (1970) W types, the more massive components have markedly lower surface brightness than expected from the gravity-darkening relation. This poorly understood flux deficit corresponds to a surface temperature roughly 4–5% (200–250 K) lower than expected. What causes this deficit? No one really knows. Spots on the primary could be the culprit in these rapidly rotating convective stars (e.g., Eaton 1986a). However, the flux deficit could actually be a signature of the envelope circulation that somehow transfers luminosity from the more massive to the less massive component.

It is clear that these stars must have some sort of circulation in their common envelopes to transfer luminosity from a more massive component to a less massive one that is radiating more luminosity than it can produce. Because their surfaces are in motion, such binaries cannot be in strict hydrostatic equilibrium but must have gravitational heads or other pressure gradients to drive and regulate the flows. In the W-type systems (cooler, convective) a surface flow from the more massive to the less massive would require the primary's surface to be higher and possibly cooler.

Can we actually know if V963 Per is a contact binary? Such binaries are characterized by how much they overfill their Roche lobes. Binnendijk's possibly radiative A-type systems tend to overfill the lobe by several tens of percent, his presumably convective W-type systems by $\lesssim$10% (e.g., Smith 1984). Solutions for stars like V963 Per tend to overfill their lobes even less, if at all. However, how much the solutions overfill the lobe depends on assumptions about limb and gravity darkening, photometric elements that might not have their theoretical values in these stars. In addition, light curve programs, such as WD, do not move seamlessly through the transition from very close detached systems, through semi-detached systems, to contact systems. Instead, they have different modes for detached, semi-detached, and contact systems.

It's gratifying that i and q did not change materially between 2011-dec and 2012-jan in spite of marked change in the light curve, nor did the temperature difference between the components. What's problematic, however, is the change in filling factor over our four epochs. Naively, the fillout might change on short timescales given the likely small thermal timescale of the common envelope, as we have argued in section 4. However, such a change in envelope thickness implies a somewhat different distribution of mass beween the components, leading to a change in the orbital period on a rather short timescale. We don't think this effect is observed in these contact binaries. So what would cause the fillout to appear to change? The results in columns 2, 6, and 7 of Table 3 suggest that spots could change the fillout derived. A cool O'Connell spot at phase 0.75 on the primary flattens out that branch of the light curve, requiring a larger distortion (more overfilling) to give the observed ellipsoidal variation at both maxima. A hot spot on the secondary at phase 0.25 (Table 3 column 6), on the other hand, makes that maximum more peaked, requiring a smaller fillout to fit the distortion around phase 0.75. This effect actually shows up in the solutions, as you can see by comparing columns 2 and 6 of Table 3.

At this point, V963 Per seems to be a genuine contact binary, overfilling its Roche lobe by 5 to 10%. But that is absurd if we believe the theoretical predictions of Lucy (1968a) and others that to be stable, two stars in contact must have a common envelope in which physical properties must be roughly uniform on equipotential surfaces to preserve (pseudo) hydrostatic equilibrium. The temperature difference $T_1 - T_2$, should also remain relatively constant, inasmuch as it represents the thermal state of the gas, for the same theoretical reason and to avoid unobserved consequences of short-term mass redistribution. To conclude, we hope this paper stimulates others of a more theoretical orientation to think about the structure and evolutionary state of these peculiar contact binaries.

6. Acknowledgements

Joel Eaton thanks Jonna Peterson and Brian Skiff for their help in locating various data and analyses Odell had done before he died in May 2019. Andy Odell would acknowledge the gracious amounts of observing time allotted to his research programs over the years by the University of Arizona and Lowell Observatory. He would also thank Patrick Wils for advice on figuring out just what SAMEC had done and Elizabeth Green for help with obtaining, reducing, and analyzing the spectra from Steward. This research used the SIMBAD database, operated at CDS, Strasbourg, France, and the SAO/NASA Astronomical Data Service.

References

Al-Naimy, H. M. 1978, *Astrophys. Space Sci.*, **53**, 181.
Banfi, M., *et al.* 2012, *Inf. Bull. Var. Stars*, No. 6033, 1.
Binnendijk, L. 1970, *Vistas Astron.*, **12**, 217.
Butters, O. W., *et al.* 2010, *Astron. Astrophys*., **520**, L10.
Diethelm, R. 2012, *Inf. Bull. Var. Stars*, No. 6029, 1.
Diethelm, R. 2013, *Inf. Bull. Var. Star*s, No. 6063, 1.
Eaton, J. A. 1986a, *Acta Astron.*, **36**, 79.
Eaton, J. A. 1986b, *Acta Astron.*, **36**, 275.
Eaton, J. A. 1991, *Astrophys. Space Sci.*, **186**, 7.
Eaton, J. A., Henry, G. W., Bell, C., and Okorogu, A. 1993, *Astron. J.*, **106**, 1181.
Eaton, J. A., Odell, A. P., and Nitschelm, C. A. 2021, *Mon. Not. Roy. Astron. Soc.*, **500**, 145.
Eaton, J. A., Odell, A. P., and Polakis, T. A. 2019, *Inf. Bull. Var. Stars*, No. 6263, 1.
Girardi, L., Bressan, A., Bertelli, G., and Chiosi, C. 2000, *Astron. Astrophys., Suppl. Ser.*, **141**, 371.
Kałużny, J. 1983, *Acta. Astron.*, **33**, 345.

Kałużny, J. 1986a, *Acta Astron.*, **36**, 105.
Kałużny, J. 1986b, *Acta Astron.*, **36**, 113.
Kałużny, J. 1986c, *Acta Astron.*, **36**, 121.
Kałużny, J. 1986d, *Publ. Astron. Soc. Pacific*, **98**, 662.
Kałużny, J., and Pojmański, G. 1983, *Acta Astron.*, **33**, 277.
Lucy, L. B. 1967, *Z. Astrophys.*, **65**, 89.
Lucy, L. B. 1968a, *Astrophys. J.*, **151**, 1123.
Lucy, L. B. 1968b, *Astrophys. J.*, **153**, 877.
Odell, A. P. 1996, *Mon. Not. Roy. Astron. Soc.*, **282**, 373.
Odell, A. P., Wils, P., Dirks, C., Guvenen, B., O'Malley, C. J., Villarreal, A. S., and Weinzettle, R. M. 2011, *Inf. Bull. Var. Stars*, No. 6001, 1.
Qian, S.-B., He, J.-J., Zhang, J., Zhu, L.-Y., Shi, X.-D., Zhao, E.-G., and Zhou, X. 2017, *Res. Astron. Astrophys.*, **17**, 87.
Ruciński, S. M. 1969, *Acta Astron.*, **19**, 245.
Ruciński, S. M. 2015, *Astron. J.*, **149**, 49.
Ruciński, S. M. 2020, *Astron. J.*, **160**, 104.
Ruciński, S. M., and Lu, W. 2000, *Mon. Not. Roy. Astron. Soc.*, **315**, 587.
Samec, R. G., Melton, R. A., Figg, E. R., Labadorf, C. M., Martin, K. P., Chamberlain, H. A., Faulkner, D. R., and van Hamme, W. 2010a, *Astron. J.*, **140**, 1150.
Samec, R. G., Melton, R. A., Figg, E. R., Labadorf, C. M., Martin, K. P., Chamberlain, H. A., Faulkner, D. R., and van Hamme, W. 2010b, *Astron. J.*, **140**, 2145.
Smith, R. C. 1984, *Q. Jour. Roy. Astron. Soc.*, **25**, 405.
van Hamme, W. 1993, *Astron. J.*, **106**, 2096.
van Hamme, W., and Cohen, R. E., 2008, in *Short-Period Binary Stars: Observations, Analyses, and Results*, ed. E. F. Milone, D. A. Leahy, D. W. Hobill, Springer, Berlin, 215.
Wilson, R. E. 1990, *Astrophys. J.*, **356**, 613.
Wilson, R. E. 1994, *Publ. Astron. Soc. Pacific*, **106**, 921.
Wilson, R. E., and Devinney, E. J. 1971, *Astrophys. J.*, **166**, 605.
Wilson, R. E., and van Hamme, W. 2015, "Computing Binary Star Observables" (https://faculty.fiu.edu/~vanhamme/binary-stars/).